Journal of Thermal Analysis and Calorimetry, Vol. 85 (2006) 2, 391–399

INFLUENCE OF H-ZSM-5, Al-MCM-41 AND ACID HYBRID ZSM-5/MCM-41 ON POLYETHYLENE DECOMPOSITION

F. S. M. Sinfrônio[1*], *A. G. Souza*[1], *Ieda M. G. Santos*[1], *V. J. Fernandes Jr.*[2], *Cs. Novák*[3] *and Zsuzsanna Éhen*[4]

[1]Departamento de Química, CCEN, Universidade Federal da Paraíba, 58059-900 João Pessoa, Paraíba, Brazil
[2]Departamento de Química, CCET, Universidade Federal do Rio Grande do Norte, Natal, Rio Grande do Norte, Brazil
[3]Hungarian Academy of Sciences, Budapest University of Technology and Economics, Research Group of Technical Analytical Chemistry, Szt. Gellért tér 4, 1111 Budapest, Hungary
[4]Institute of General and Analytical Chemistry, Budapest University of Technology and Economics, Szt. Gellért tér 4 1111 Budapest, Hungary

Thermogravimetry (TG) and mass spectrometry (MS) combined techniques have been used to investigate the thermal degradation and catalytic decomposition of high-density polyethylene (HDPE) over solid acid catalysts as H-ZSM-5, Al-MCM-41 and a hybrid material with a bimodal pore size distribution (H-ZSM-5/AL-MCM-41). The silicon/aluminum ratio of all catalysts is 15. Both thermal and catalytic processes showed total conversion in a single mass loss step. Furthermore, the catalytic conversion presents average reduction of 27.4%, in the onset decomposition temperature. The kinetic parameters were calculated using non-isothermal method. These parameters do not indicate significant differences between the thermal and catalytic processes. Even though, the presence of the catalysts changes the reaction mechanism, from phase boundary controlled reaction to random nucleation mechanism. Important difference in distribution of evolved products was detected when several catalysts were used. However, in all cases the main products were alkanes (C_2, C_3 and C_4), alkenes (C_3 and C_4), dienes (C_4 and C_5) and traces of aromatic compounds.

Keywords: *HDPE, kinetic parameters, mass spectrometry, thermogravimetry, zeolitic materials*

Introduction

The accumulation of a high amount of plastics wastes has a negative implication on the environment. Several times these wastes are disposed on landfills or incineration areas, leading to serious environmental troubles due to its low biodegradability, and also, emission of the toxic chemical gases during the incineration process. Nowadays, in Brazil, about 2.5 million tones of residue is produced per year (US$ 4.6 billion/year), from which, only 20% is financially explored [1].

There are various methods employed to recycle polymer, being classified as: primary (extrusion), secondary (mechanical recycling), ternary (chemical or thermal recycling) and quaternary (incineration). Thermal degradation process, used in ternary recycling, requires high temperature and gives a wide range of products. On the other hand, catalytic degradation provides control of both the yielded product and distribution, reducing significantly the degradation temperature.

In recent years, important works have been published on the thermal and catalytic degradation over solid acid catalysts, such as, amorphous silica-alumina, and zeolites, as HY, MCM-41 and ZSM-5 [2–4]. However, few works discussed the effect of chemical and nanostructured structural modification on material properties. It was already observed that microporous molecular sieves, such as the ZSM-5 zeolite, present potential use as acid catalyst, for its abundant uniform microporous structures and strong intrinsic acidity. Conversely, because of the small pore sizes, such microcrystalline materials cannot effectively react with large molecules [5]. On the other hand, mesoporous molecular sieves, as MCM-41 have a high thermal stability and strong superficial acidity [6], but demonstrate lower catalytic activity due to its amorphous framework characteristics. This way, the application of zeolitic materials with bimodal pore size distribution (meso and micropores) can solve the above listed disadvantages, combining the benefits of both materials [7]. Application of these kinds of materials can improve the conversion of waste plastics into hydrocarbon mixtures, in the form of gas, or liquid products in gasoline boiling range.

Together with the development of new materials, the optimization of the catalytic degradation procedure should be based on the relation between the chemical composition of yielded degradation products and the kinetic/thermodynamic parameters. In this context, this work aims to evaluate the influence

* Author for correspondence: kjvida@terra.com.br

1388–6150/$20.00

Akadémiai Kiadó, Budapest, Hungary
Springer, Dordrecht, The Netherlands

of the acid ZSM-5, Al-MCM-41 and composites (all with silicon/aluminum ratio equal to 15) on the thermal degradation of the high-density polyethylene under non-isothermal conditions, by means of TG-MS combined technique.

Experimental

Materials

The acid ZSM-5 (HZ) were synthesized by hydrothermal method, according to the procedure described by Souza *et al*. to obtain a gel with 10.60TPABr: $3.33Al_2O_3$:$14.3Na_2O$:$100.00SiO_2$:$2000.00H_2O$ [7]. Aluminum-containing MCM-41 (AlM) was prepared using the method previously proposed by Araujo *et al*., with a composition of 1.00CTMABr:$0.13Al_2O_3$:$1.06Na_2O$:$4.00SiO_2$:$200.00H_2O$ [8]. The acid form of the hybrid material, H(ZM), was synthesized as proposed by Huang *et al*., in which the molar composition of the gel is 0.20TPABr:0.16CTMABr:$0.03Al_2O_3$:$0.32Na_2O$:$1.00SiO_2$:$55.00H_2O$ [9].

The high-density polyethylene (HDPE) sample was obtained from Brazilian industries, in the form of granules (pellets), without inorganic additives.

The evaluation of the thermal degradation of all polymers, and also, the catalytic degradation were carried out using TA 2920 TMDSC (TA Instruments) under flowing nitrogen atmosphere (50 mL min^{-1}), at a heating rate of 5, 10 and 20 K min^{-1}, aluminum pans, sample mass of approximately 5.0 mg, in the range of 30–400ºC.

X-ray diffraction characterization of the zeolitic materials was done by a Shimadzu XRD-6000 powder X-ray diffractometer using CuK_α radiation. The FTIR spectra were obtained in the range of 4000–400 cm^{-1} using a BOMEM MB-102 infrared spectrometer, using KBr pellet technique.

The thermal degradation of the polymer was studied using STD 2960 simultaneous TG-DTA unit (TA Instruments) using alumina pan, applying β= 10 K min^{-1} heating rate and helium purging (100 mL min^{-1}). For evaluation of the evolved gases, the STD 2960 unit was connected to a Balser Thermostar GSD 300T quadrupole mass spectrometer. Evolved gases were transferred through a heated silica capillary (capillary temperature was 200ºC). The use of *m*/*e*=43 for *n*-propane instead of *m*/*e*=44 is to avoid the interference with the signal of CO_2, and the use of *m*/*e*=27 instead of *m*/*e*=28 for ethylene is to avoid the interference from CO.

Modeling of kinetics parameters

All kinetics studies were based on the correlation of TG experimental data with kinetic expressions, in which the degree of conversion (α) is expressed as:

$$\alpha = \frac{w_i - w}{w - w_f} \quad (1)$$

where for non-isothermal experimental conditions, w is the actual mass, w_i is the mass at the beginning of the decomposition and w_f is the mass at the end of the mass loss event.

The rate equation of conversion can be expressed as:

$$\frac{d\alpha}{dT} = A e^{-\frac{\Delta E_a}{RT}} (1-\alpha)^n \quad (2)$$

where A is the frequency factor (s^{-1}), n is the overall reaction order, E_a is the apparent activation energy (J mol^{-1}), R is the gas constant (8.314 J mol K^{-1}), T is the reaction temperature (K) and $(1-\alpha)$ is the amount of remaining polymer.

In integral methods, the Eq. (2) is used as:

$$\frac{d\alpha}{(1-\alpha)^n} = \frac{A}{\beta} e^{-\frac{E_a}{RT}} dT \quad (3)$$

where β is the heating rate (K min^{-1}).

Integrating from the starting condition of α=0 to T=T_0, the following expression is obtained:

$$F(\alpha) = \int_0^\alpha \frac{d\alpha}{(1-\alpha)^n} = \frac{A}{\beta} \int_{T_0}^{T} e^{-\frac{E_a}{RT}} dT \quad (4)$$

One of the most often used integral methods was proposed by Coats–Redfern, in which an asymptotic approximation is used to solve Eq. (4), obtaining Eq. (5) [10]:

$$\ln \frac{F(\alpha)}{T^2} = \ln \frac{AR}{\beta E_a} - \frac{E_a}{RT} \quad (5)$$

The expressions of $F(\alpha)$ for different mechanism were presented in previous papers [11, 12], and the activation energy for each degradation mechanism can be obtained from the slope of $F(\alpha)/T^2$ *vs*. $1000/T$ plot.

Another integral method was developed by Madhusudanan, in order to estimate the kinetic parameters from the TG/DTG curves [13]. In this case, the activation energy can be calculated from Eq. (6), when describing the left side of Eq. (6) *vs*. reciprocal temperature results a straight line. So, E_a and A can be calculated from the slope and the intercept.

$$\ln\left[\frac{1-\ln(1-\alpha)}{T^{1.9206}(1-n)}\right]=\ln\frac{AR}{\beta R}+0.02-$$
$$-1.9206\ln\frac{E_a}{R}-0.12040\frac{E_a}{RT} \quad (6)$$

The Van Krevelen method is based on the use of the temperature (T_{max}) at which the rate is maximum. For the temperature range between $0.9T_{max}<T<1.1T_{max}$, the following approximation can be assumed [14]:

$$\ln F(\alpha)=\ln\left[\frac{A}{\beta}\left(\frac{0.368}{T_{max}}\right)^{\frac{E_a}{RT_{max}}}\left(\frac{1}{\frac{E_a}{RT_{max}}+1}\right)\right]+$$
$$+\left(\frac{E_a}{RT_{max}}+1\right)\ln T \quad (7)$$

Throughout the plot of $\ln F(\alpha)$ *vs*. $\ln T$, the activation energy is calculated using the resultant slope. In this method only the relative mass of the sample is required as a function of reaction temperature.

An alternative method for calculating activation energies according to the best linear plot was proposed by Horowitz–Metzger [15], which used an approximate integration of the rate equation. In this method, $-\ln(1-\alpha)$ is plotted *vs*. β, resulting in a straight line whose slope is E_a/RT. The activation energy is calculated from the slope as follows:

$$\ln\left[\frac{1-(1-\alpha)^{1-n}}{1-n}\right]=\frac{E_a\beta}{RT_s} \quad (8)$$

where T_s is the peak temperature of the DTG curve.

Results and discussion

Material characterization

The DSC curves obtained by temperature modulated technique are presented in Fig. 1.

The TMDSC curve (refers to the melting of the polymer, see peak at 131°C) is in good agreement with the data reported in [16]. The sharp endotherm peak indicates high level of purity for this polymer.

Figure 2 compares the XRD patterns of the micro- (Fig. 2A) and mesoporous (Fig. 2B) materials to the pattern of the composite. The observed peaks confirm the formation of the desired phases. These peaks are characteristic for long-range ordered hexagonal structure. The XDR patterns of H(ZM) sample are similar to the H-ZSM-5 and Al-MCM-41, presenting almost the same reflections. It can be inferred that the hexagonal mesostructure of the Al-MCM-41 is preserved although the intensities of the corresponding diffraction peaks (110) and (200) were reduced. Conversely, there is a significant reduction in the apparent

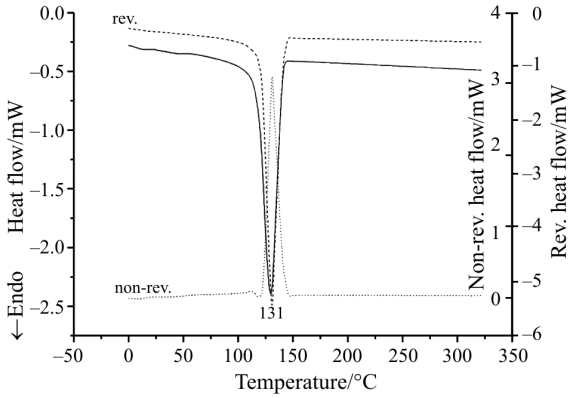

Fig. 1 TMDSC curves of HDPE

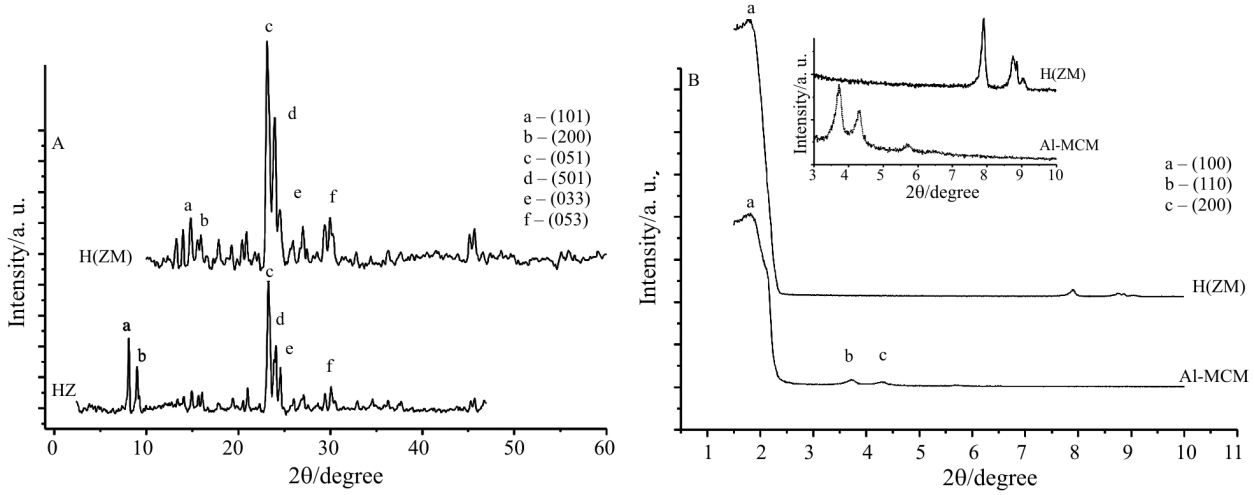

Fig. 2 A – XRD patterns of HZ and H(ZM), B – low-angle XRD patterns of Al-MCM and H(ZM)

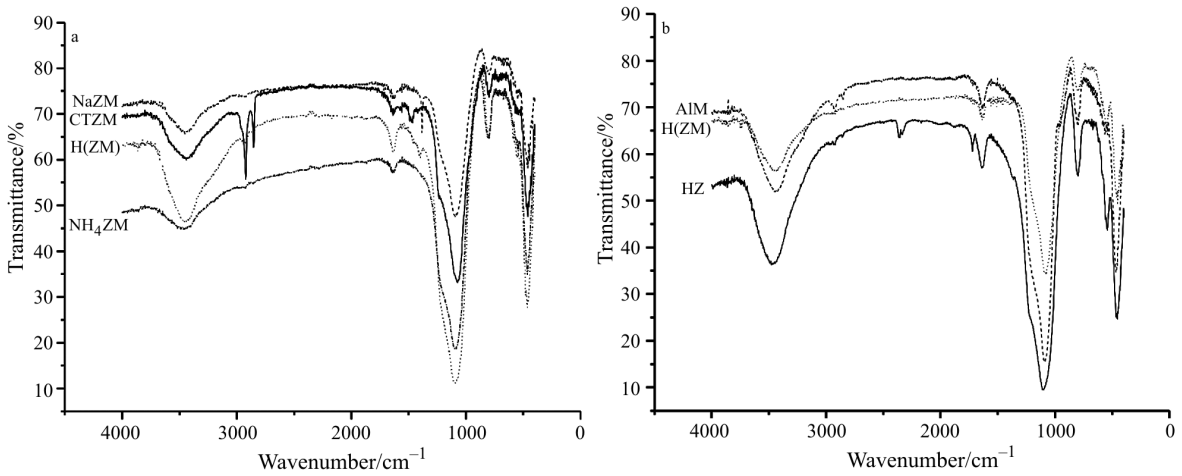

Fig. 3 FTIR spectra of a – ZSM-5/MCM-41 composite during synthesis processes and b – comparison of several catalyst spectra

crystallinity of the microporous material, as well as, a shift of peaks to small crystal planes, due to the change in the microstructural symmetry.

Figure 3a shows the FTIR spectra of the H(ZM) and the precursors, which are as-synthetized (TZM), calcined (NaZM), ion-exchanged (NH_4ZM) and calcined after ion-exchanging (H(ZM)). These spectra show the appearance and disappearance of absorption bands during the process of synthesis.

The hybrid material, in as-synthesized form, exhibits similar absorption bands for micro- and macroporous materials. A broad band around 3441 cm^{-1} corresponds to siloxane groups and/or hydroxyl groups of physisorbed water, whereas, bands around 2919 and 2850 cm^{-1} may be attributed to its stretching (C–H) of surfactant ions TPA^+ and $CTMA^+$. The bands around 1637 cm^{-1} are assigned to deformational vibrations of adsorbed water molecules. The bending (C–H) vibration of methyl group of the surfactant ions arises around 1473 cm^{-1}. The bands around 1238 and 1070 cm^{-1} may attribute to external and internal asymmetrical stretching for siloxane groups, respectively. Symmetric stretching is observed around 719 and 544 cm^{-1} due to siloxane groups. The band around 459 cm^{-1} is assigned to tetrahedral bending modes. The presence of bands around 544 and 459 cm^{-1} is a strong evidence that crystalline ZSM-5 framework was structured [17].

Table 1 summarizes the most representative bands and their assignments of used surfactants to the synthesis of catalysts in their as-synthesized forms. Nevertheless, only small differences in the band positions are observed between the samples.

Catalyst evaluation

Thermal analysis

Thermal analysis was carried out to determine the thermal stability of the HDPE over several catalysts. The thermal behavior of the polyolefin and their respective mixtures (1:1 mass/mass) with the acid zeolitic materials (Si/Al=15) are illustrated in the Figs 4a and b. The TG profile of pure HDPE and HDPE/catalyst samples exhibited just a single mass loss step, when all polyolefin is converted. In the polymer/zeolite system, the onset decomposition temperature is shifted towards lower values than in polymeric cracking, changing from 408.4 to 346.6°C (HZ), 363.1°C (AlM) and 344.2°C (H(ZM)). According to the DTG curves (Fig. 4a), it can be inferred that the maximum conversion temperature of pure polymer 486.0°C, decreases to 398.9°C (HDPE/HZ), 430.5°C (HDPE/AlM) and 413.3°C (HDPE/H(ZM)) for sample mixtures. The DTA peak around 130°C refers to the melting of the polymer. The TG and DTG curves show that the thermal behavior of the polymer/composite system is be-

Table 1 Frequencies and suggested band assignments of as-synthesized catalysts

Sample	Region/cm^{-1}										
attribution	ν_{O-H}	ν_{C-H}		δ_{O-H}	ν_{C-H}	$\nu_{a(Si-O-Si)}$		ν_{Si-O^-}	$\nu_{s(Si-O-Si)}$		$\delta_{Si-O-Si}$
TZ	3463	2920	2852	1635	1458	1224	1101	995	792	541	464
CM	3446	2925	2855	1631	1482	1230	1081	966	796	557	463
CTZM	3441	2919	2850	1637	1473	1238	1070	–	719	544	459

TZ – tetraethylammonium-ZSM-5, CT – cetyltrimethylammonium-MCM-41,
CTZM – (cetyltrimethylammonium/tetraethylammonium)-ZSM-5/MCM-41

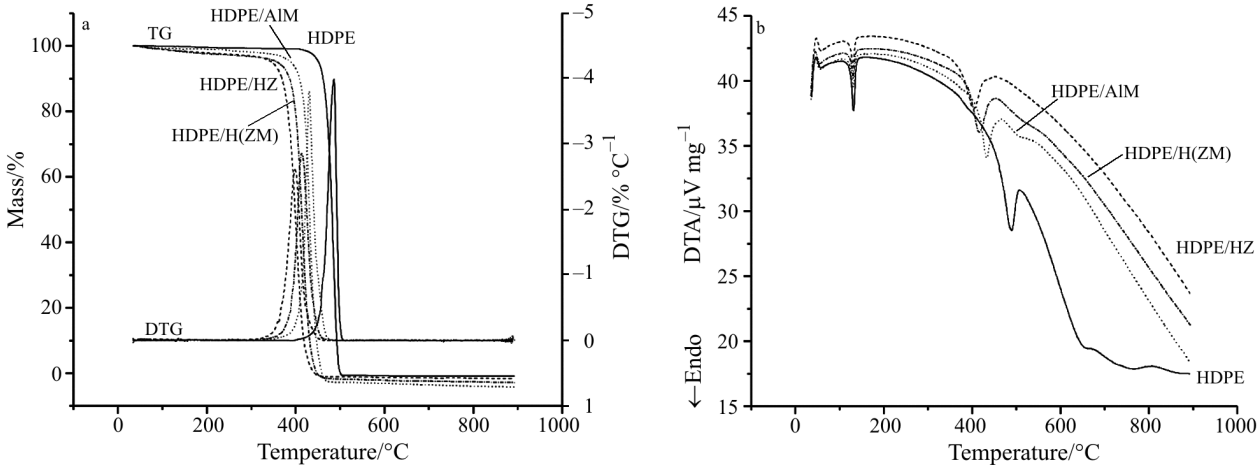

Fig 4 a – TG/DTG and b – DTA curves of HDPE and HDPE/catalyst systems

tween the micro- and mesoporous process. Such behavior indicates that the catalytic properties of the composite are closely related to its bimodal pore distribution. For all cases, as expected, the polymeric and catalytic conversion is an endothermal process (Fig. 4b). Based on the thermogravimetric data, the thermal stability of mixtures in the catalytic process can be assumed as: H-ZSM-5>H(ZM)>Al-MCM-41.

In order to quantify the overall activation energy, approximate and integral algorithms were used. Table 2 presents the kinetics parameters, and their respective linear regression coefficients, both for the polymer and polymer/zeolite mixtures using Coats–Redfern (CR), Madhusudanan (MD), Horowitz–Metzger (HM) and Van Krevelen (VK) methods, under non-isothermal conditions.

The activation energy values obtained by MD, HM, and VK methods for HDPE/HZ sample are very close, except for the HDPE/AlM sample. For other systems a discrepance between the kinetics parameters is observed. As a general rule, all obtained parameters are slightly higher than those reported in literature [14], as a consequence of the higher heat conductivity of helium (purge gas) compared to nitrogen. In the majority of the cases, the integral model proposed by Madhusudanan is the best to predict the kinetic parameters, however, the values calculated using Coats–Redfern method are higher than expected. Probably for asymptotic approximation used to solve the integrated conversion equation. The Horowitz–Metzger and Van Krevelen models are not able to calculate the frequency factor and the overall reaction order of the Al-MCM-41 system.

The degradation mechanisms were evaluated using different kinetic models proposed in the literature [18]. Table 3 summarizes the activation energies obtained for degradation. The degradation of polymers is a complex phenomenon which involves several parallel reactions. The individual contribution of each one of these reactions, to the overall degradation process, may not be quantified. For this reason, a straight deviation on the global mechanism parame-

Table 2 Kinetic parameters of catalytic degradation of HDPE and HDPE/H-MCM-41-ZSM-5 samples

Kinetic method	Sample	n	E_a/kJ mol^{-1}	A/s^{-1}	r
CR	HDPE	0.49	415.77	$5.3\cdot10^{26}$	0.9995
	HDPE/HZ	1.43	300.89	$2.4\cdot10^{21}$	0.9994
	HDPE/AIM	1.79	502.30	$3.0\cdot10^{35}$	0.9994
	HDPE/H(ZM)	1.57	372.18	$2.5\cdot10^{26}$	0.9990
MD	HDPE	0.30	393.63	$1.4\cdot10^{25}$	0.9985
	HDPE/HZ	1.42	299.85	$2.1\cdot10^{21}$	0.9992
	HDPE/AIM	1.89	521.04	$8.4\cdot10^{36}$	0.9996
	HDPE/H(ZM)	1.49	352.43	$7.1\cdot10^{24}$	0.9986
HM	HDPE	0.53	443.34	$5.2\cdot10^{28}$	0.9994
	HDPE/HZ	1.46	317.56	$5.8\cdot10^{22}$	0.9996
	HDPE/AIM	1.97	–	–	0.9989
	HDPE/H(ZM)	1.62	392.75	$1.1\cdot10^{28}$	0.9996
VK	HDPE	0.44	417.17	$3.7\cdot10^{32}$	0.9960
	HDPE/HZ	1.49	302.01	$1.4\cdot10^{27}$	0.9815
	HDPE/AIM	1.93	–	–	0.9978
	HDPE/H(ZM)	1.55	336.05	$1.8\cdot10^{29}$	0.9448

Table 3 Activation energy and decomposition mechanism of HDPE and HDPE/catalyst samples obtained by Coats–Redfern method

Mechanism	HDPE		HDPE/HZ		HDPE/AIM		HDPE/H(ZM)	
	E_a/kJ mol^{-1}	r	E_a/kJ mol^{-1}	r	E_a/kJ mol^{-1}	r	E_a/kJ mol^{-1}	r
A2	230.52	0.9993	134.82	0.9999	217.14	0.9992	166.25	0.9997
A3	151.61	0.9993	88.05	0.9999	142.83	0.9992	108.96	0.9997
A4	112.16	0.9993	64.67	0.9999	105.67	0.9992	80.31	0.9997
D1	773.48	0.9993	482.19	0.9997	720.71	0.9948	580.53	0.9992
D2	824.48	0.9999	505.37	0.9999	770.77	0.9970	612.10	0.9996
D3	881.66	0.9999	530.31	1.0000	827.39	0.9987	646.59	0.9998
D4	843.48	1.0000	513.67	1.0000	789.58	0.9980	623.58	0.9998
F1	467.24	0.9993	275.13	0.9999	440.10	0.9992	338.13	0.9997
F2	175.89	0.9465	72.23	0.9715	175.36	0.9457	102.60	0.9604
F3	357.99	0.9465	149.94	0.9715	356.53	0.9457	210.84	0.9604
P2	230.52	0.9986	134.82	0.9995	217.14	0.9896	166.25	0.9984
P3	123.74	0.9986	75.79	0.9995	115.28	0.9896	92.06	0.9984
R1	383.64	0.9986	238.35	0.9995	357.45	0.9896	287.45	0.9984
R2	423.59	0.9999	256.23	1.0000	396.80	0.9964	311.93	0.9996
R3	437.73	0.9997	262.41	1.0000	410.79	0.9974	320.48	0.9997

ters compared to the thermodynamic data is observed. Regarding to the decomposition mechanism, it was observed that the process changes from phase boundary controlled reaction with contracting area (R2), in the polymeric cracking, to random nucleation mechanism with one single nucleus (F1), in the catalytic conversion for all materials (Table 3). Such result indicates that the reaction mechanism has small correlation with diffusional factors (mass transfer), since no imperative distinction was established among the different catalysts.

Mass spectrometric results

Previous study concerning the thermal degradation of polyethylene had shown that this process leads to the random scission of the polymer chain, throughout parallel processes, producing mainly C_1–C_8 hydrocarbons, such as: alkanes and alkenes [19]. Besides, a couple of dienes, trienes and aromatic compound are also produced.

In order to obtain further information concerning possible modification in the composition of the formed products during the catalytic degradation, TG/MS combined technique was applied. The mass spectrometric behavior of all investigated samples (Fig. 5) indicates the formation of similar fragments in the low specific mass/charge (m/e) range.

At the beginning of the catalytic conversion, the lower fragments, can be attributed to H_2O (m/e=18) and O_2 (m/e=32) molecules due to their desorption from the surface of catalyst. Conversely, during the decomposition process, the ionic fragment at m/e=28 resulted from the production of ethane and also a less amount of CO. It is also important mentioning that other fragments were detected over 110 amu, but they were omitted for their infinitesimal amount compared to the fragments with lower masses. It may be observed that all catalysts modified the fragments distribution.

The SAC curves (Fig. 5) indicate that the HDPE thermal degradation occurs with the formation of a high amount of fragments in the 10–20 and 25–35 amu range. In addition, a large number of fragments were also detected around 50–75 amu and fragments with higher masses were observed between 80 and 102, whereas, just traces of high mass fragments appear around 105 amu. These results indicate that a wide range of compounds is produced. Majority of these fragments contains relative low amu, indicating a favorable cleavage in the terminal groups of the polymeric chain at the beginning of the decomposition. During the conversion with H-ZSM-5 there was a slight increase in fragments at 35–45 amu, whereas, at 50–60 amu a significant rise was observed. Over 60 amu the ion current decreased, compared to previous processes, probably due to the restricted channel and pore volumes (pentasil rings). The Al-MCM-41 demonstrated similar behavior to microporous material in low m/e range. On the other hand, a strong selectivity towards high mass fragments was observed, mainly in the range of 50–84 amu, due to its structural arrangement. In contrast, this catalyst almost did not change the fragments distribution to species higher than 105 amu. When the hybrid material was used, a meaningful improvement occurred between 35 and 45 amu, instead of the straight reduction to heavy ionic fragments in comparison to the macroporous cata-

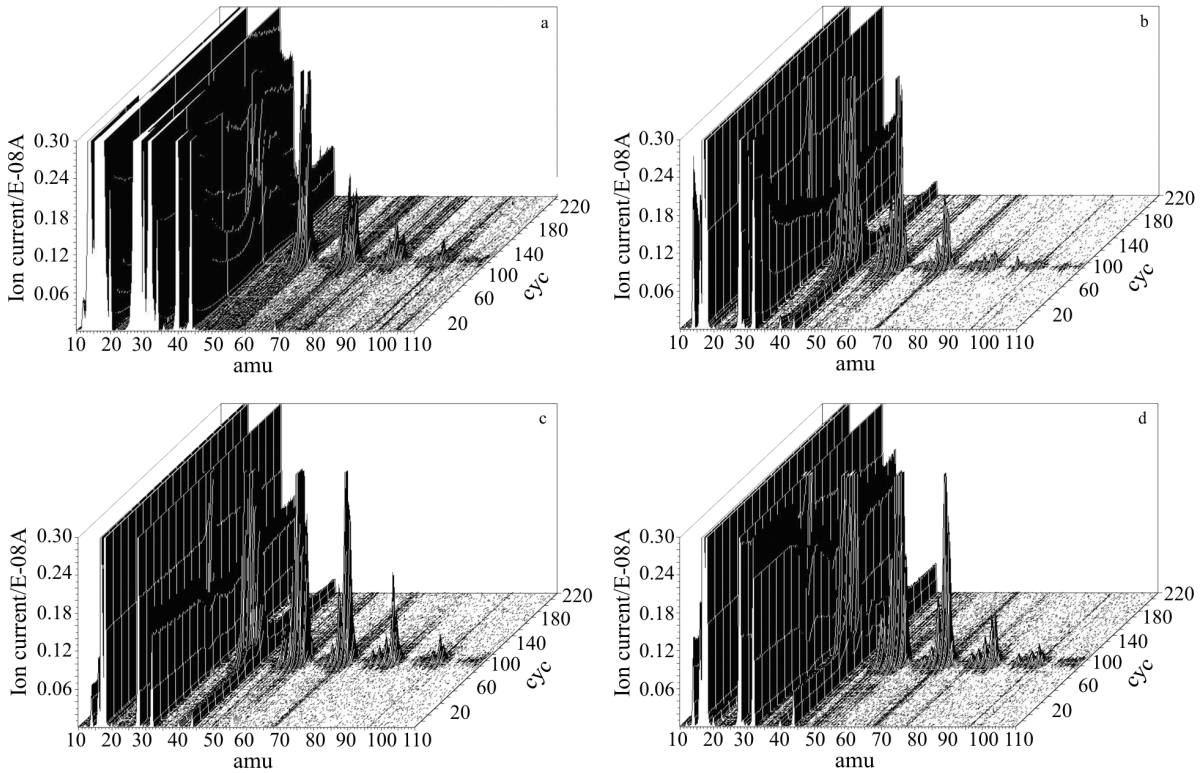

Fig. 5 Mass spectrometric behavior of the a – HPDE and mixtures with b – H-ZSM-5, c – Al-MCM-41 and d – H(ZM)

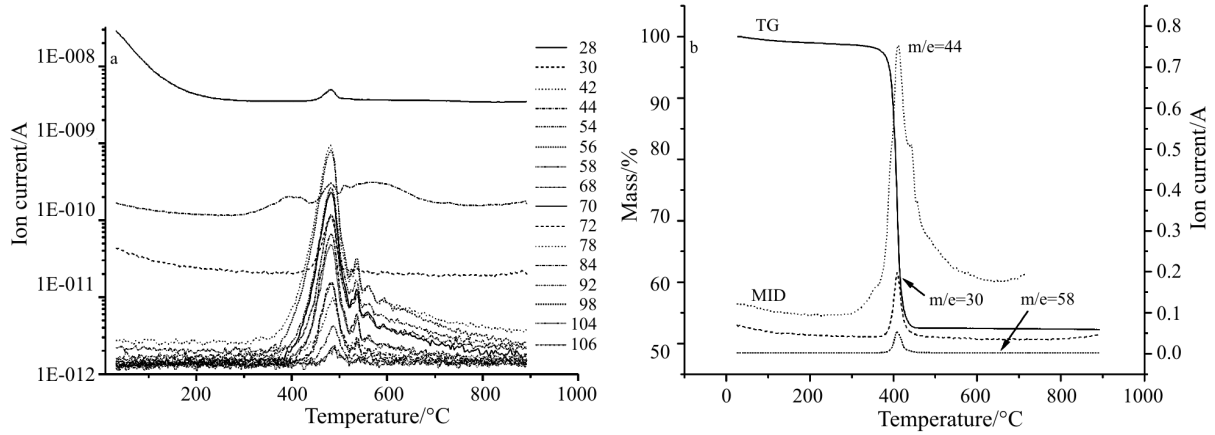

Fig. 6 a – MID curves and b – TG and MID curves as a function of temperature, of HDPE

lyst. That effect comes from the steric and diffusional limitation for the access of the reactant molecules to the acidic sites of catalyst.

The ion currents were also continuously recorded for previously selected mass numbers (MID). Figure 6a illustrates the MID curves of the HDPE/composite.

The MID measurement (Fig. 6a) showed that in the decomposition range different fragments are detected almost at the same time. It can be attributed to the similarity of the hydrocarbons formed during the cleavage of the polymeric chain or recombination of lower fragments in the detector of the mass spectrometer. By the comparison of MID curves it could be observed that for all HDPE/catalyst samples the volatile products evolved at lower temperature compared to the free radical cracking. Figure 6b illustrates the distribution of the same fragments along the decomposition process, as well as, the congruence between the maximum values of conversion in DTG (Fig. 4a) and MID curves. That is an important fact because it makes possible to quantify the fragments through the maximum ion currency, as it is shown in Fig. 7.

The mass spectra of the polymer, as well as sample/catalyst samples demonstrated that a large range of compounds are produced almost at same time during the degradation process (Fig. 6b). This fact could be

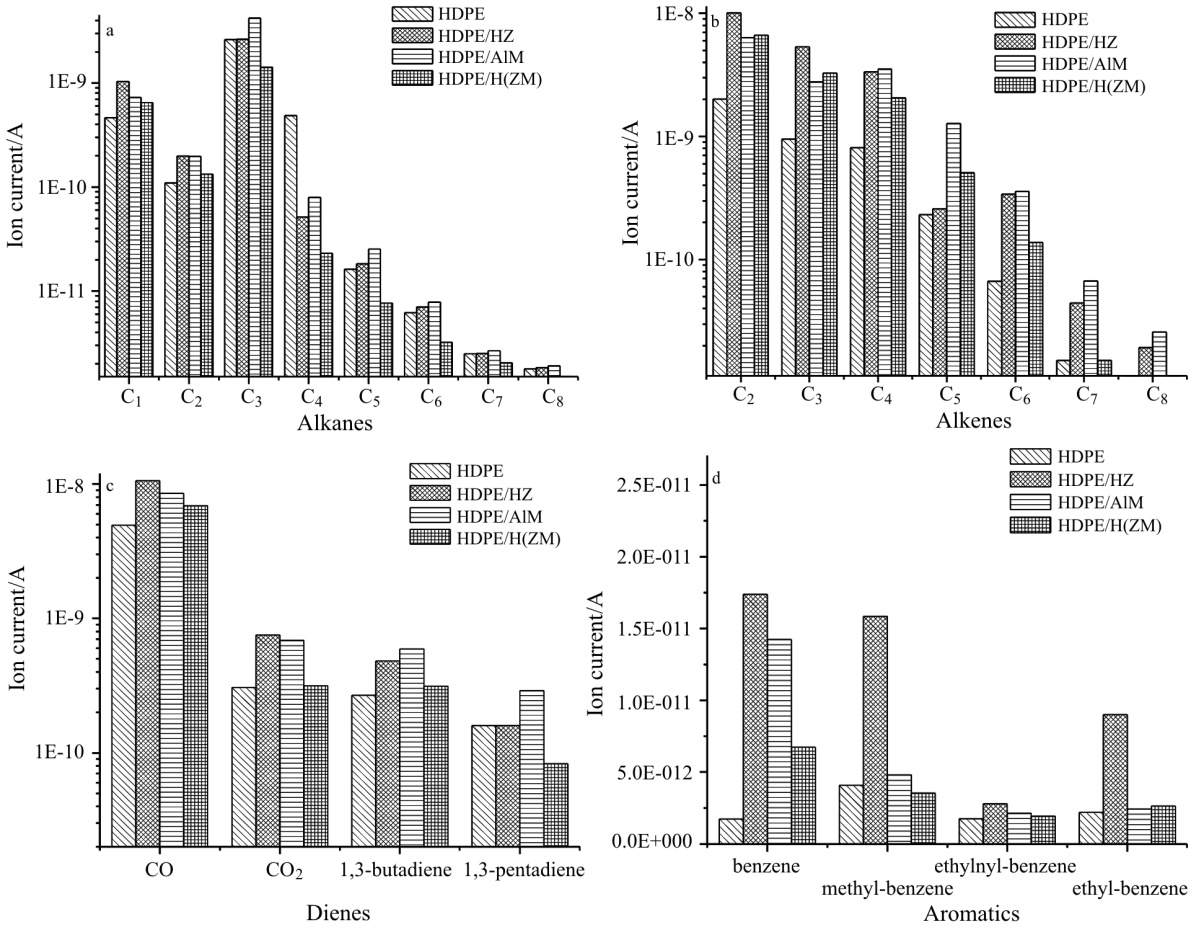

Fig. 7 Class-specific ion current profiles of HDPE/catalyst samples for a – alkanes, b – alkenes, c – CO, CO_2, dienes and d – aromatic compounds

understood based on the carbenium ion species formed from polymer chain fragmentation, either at random or terminal positions. Once formed, they could be subject to a wide number of reactions, including β-cracking, hydride transfer, isomerization, cyclization and aromatization. Thus, it is predictable that light olefins, isoparaffins and aromatics can be yielded.

The degradation of the pure HDPE clearly exhibited a selectivity towards alkene compounds (from C_2 up to C_6), in which ethylene, *n*-propene and *n*-butene are extensively formed. Even thought, CO, CO_2 and several alkanes (e.g. ethane and *n*-propane also detected in appreciable quantity. One reason to that is because of the weak transfer of intermolecular hydrogen a few portion of alkenes are saturated to paraffins. The formation of diene fragments, in all cases, indicates that some fragments undergo stabilization by resonance during the propagation step. In addition, the formation of diene compounds essentially is not modified by the catalysts used. In all experiments, it was observed that the proportion of aromatic fragments is relatively low, in which rather benzene and alkylbenzenes are the representative products. The acid ZSM-5 increases the amount of CO, CO_2 and methane, but decreases the formation of *n*-propane, compared to the conversion of the pure polymer. Conversely, this catalyst increases twice the formation of ethylene and *n*-propene, elevating either the *n*-butene formation. Concerning the aromatic compound, the ZSM-5 has demonstrated a good shape-selective activity due to the localization of its acid sites into restricted cavities.

The Al-MCM-41 leads the cracking process to the formation of wide range of compounds, increasing also the amount of heavy fragments. This material promotes a slight decrease in CO and CO_2 formation, not affecting dramatically the alkane production. On the other hand, this molecular sieve strongly elevates the quantity of *n*-propane, ethylene, *n*-propene and *n*-butene. The highest amount of heavy fragments was observed when this kind of catalyst was used because its pore distribution.

The hybrid catalyst considerably reduces the amount of CO and CO_2 and demonstrates similar selectivity to light alkenes compared to the other catalysts. For the composite, in most cases the ion current values belonging to the same fragments were between

the ion current values which have been recorded for the application of micro- and mesoporous materials. This result is in agreement with the previously presented thermal and kinetic data.

Conclusions

The results showed that it is possible to use HDPE waste as source of gaseous and liquid hydrocarbon products by means of several catalysts. The application of the three catalysts did not affect remarkably the fragmentation of HDPE; however, the decrease of the activation energy was well pronounced. By the comparison of catalysts, their selectivity are close together. The kinetics of the thermal and catalytic conversion of HDPE can be satisfactorily evaluated by non-isothermal methods. The activation energy has been reduced in the catalytic process. Depending on the used catalyst the initial decomposition temperature of HDPE has decreased from 408 to 340–360°C. The degradation mechanism in solid state was modified in the catalytic process, from R2 to F1. The products of catalytic and thermal cracking are mainly light hydrocarbons (substantially ethylene, *n*-propane and *n*-propene) and low amount of C_6–C_8 aromatics.

Acknowledgements

The authors acknowledge CNPq and CAPES for the financial support.

References

1 S. Ucar, S. Karagoz, T. Karayildirim and J. Yanik, Polym. Degrad. Stab., 75 (2002) 161.
2 C. Vasile, P. Onu, V. Barboiu, M. Sabliouschi and G. Moroi, Acta Polym., 36 (1985) 543.
3 S. R. Ivanova, E. F. Gumerova, K. S. Minsker, G. E. Zaikov and A. A. Berlin, Prog. Polym. Sci., 15 (1990) 193.
4 A. R. Songip, T. Masuda, M. Kuwahara and K. Hashimoto, Energy Fuels, 8 (1994) 136.
5 A. Corma, Chem. Rev., 97 (1997) 2373.
6 K. R. Kloetstra, H. W. Zandbergen, J. C. Jansen and H. van Bekkum, Microporous Mater., 6 (1996) 287.
7 J. G. A. Pacheco Filho, E. C. Graciliano, A. O. S. Silva, M. J. B. Souza and A. S. Araujo, Catal. Today, 107–108 (2005) 507.
8 A. S. Araujo, V. J. Fernandes Jr., S. A. Araujo and M. Ionashiro, Stud. Surf. Sci. Catal., 141 (2002) 473.
9 L. Huang, H. Chen and Q. Li, Chinese Pat. Appl., # 981109349, (1999).
10 A. Coast and J. Redfern, Nature, 201 (1964) 68.
11 X. L. Wang, Y. Z. Wang, B. Wu, Y. D. Jin, K. K. Yang and B. Yang, Eur. Polym. J., 39 (2003) 1567.
12 J. C. O. Santos, I. M. G. Santos and A. G. Souza, J. Therm. Anal. Cal., 75 (2004) 429.
13 P. M. Madhusudanan, K. Krishnan and K. N. Ninan, Thermochim. Acta, 221 (1993) 13.
14 F. S. M. Sinfrônio, J. C. O. Santos, L. G. Pereira, A. G. Souza, M. M. Conceição, V. J. Fernandes Jr. and V. M. Fonseca, J. Therm. Anal. Cal., 79 (2005) 393.
15 H. H. Horowitz and R. Metzger, Anal. Chem., 35 (1963) 1964.
16 Polymer Handbook, 2nd Edn, Eds: J. Brandrup and E. H. Immergut, John Wiley and Sons, New York 1995.
17 P. A. Jacobs, H. J. Beyer and J. Valyon, Zeolite, 1 (1981) 161.
18 E. G. Prout and F. C. Tompkins, Trans. Faraday Soc., 40 (1944) 485.
19 L. Ballaice, Fuel, 80 (2001) 1923.

Received: February 17, 2006
Accepted: March 17, 2006

DOI: 10.1007/s10973-006-7535-0